Vuckovic et al. Supplementary data

Vuckovic et al. Supplementary Materials and Methods

Fluorescence flow cytometry analyses

Monoclonal antibodies (mAbs) used for fluorescence flow cytometry are listed in Supp. Table 1. Cells were acquired using a BD FACSCanto™ or LSRFortessa II flow cytometer (BD Biosciences, NJ, USA) and data analyzed using FlowJo software version 10.0.8r1 (BD Biosciences).

Oligoclonal expansions were defined in relation to the mean frequency of that TCR-Vβ family within the PB-$CD8^+T_N$ compartment of age-matched healthy blood donors, indicative of normal TCR-Vβ family usage during generation of the T cell repertoire.

Mass cytometry staining and data acquisition

All metal-conjugated mAbs were validated, pre-titered and supplied in per-test amounts by the Ramaciotti Facility for Human Systems Biology Mass Cytometry Reagent Bank. Reagent bank mAb were either purchased from Fluidigm® in pre-conjugated form or in a carrier-protein-free form and conjugated by the Ramaciotti Facility for Human Systems Biology with the indicated metal isotope using the MaxPAR conjugation kit (Fluidigm®, South San Francisco, CA) according to the manufacturer's protocol. Cells were fixed overnight in 4% paraformaldehyde supplemented with a DNA intercalator (0.125 μM 191/193-Iridium; Fluidigm®) followed by two washes in FACS buffer and two in MilliQ water. Cell concentration was adjusted to 0.8×10^6 cells/mL in MilliQ water supplemented with EQ beads (Fluidigm®, 1 in 10 vol/vol) and filtered through a 35 μm nylon mesh. Signal was normalized to signal intensity of the EQ beads, recorded by the in-built Helios software and exported to .fcs file for further analysis.

Analysis of mass cytometry data

FlowSOM and tSNE algorithms were run using mass cytometry data selected for minimal batch fluctuation and included matched BM and PB samples from 3 MGUS and 5 NDMM patients. Data were further interrogated by manual gating utilizing all available mass cytometry data from paired BM and PB of the total MGUS (n = 4) and NDMM (n = 8) patients. The data were randomly down sampled to 6504 cells (based on the smallest size of the T_{TE} compartment among all samples (n = 16) to ensure that there was no bias between samples. The FlowSOM algorithm (FlowSOM_seed = 45, FlowSOM_meta_seed = 9) was applied to the concatenated data (16 samples x 6504 cells = 104,064 cells), classifying cells initially into 100 clusters and

subsequently into 25 meta clusters (MC) based on the median signal intensity of 15 antigens associated with T cell differentiation and function (Supp. Table 2). The same concatenated data used for FlowSOM were used to create tSNE plots with the following parameters: perplexity = 30, theta = 0.5 and 1,000 iterations.

Vuckovic et al. Supplementary Tables

Supp. Table 1. List of mAbs used in fluorescence flow cytometry

Antigen	Clone	Supplier
CD3 V500	UCHT1	BD
CD4 PerCP-Cy5.5	SK3	BD
CD8 APC-H7	SK1	BD
CD28 APC	CD28.2	BD
CD45RO PE-Cy7	UCHL-1	BD
CD57 eFluor 450	TB01	eBiosciences
CD69 APC	FN50	BD
CD103 PE	Ber-ACT8	BD
IFN-γ APC	6401.1111	BD
TNF-α	4S.B3	BD
Cleaved Caspase3 AF488	D175	Cell Signalling Technology
Rabbit mAb IgG AF488	DA1E	Cell Signalling Technology
CD3 PerCP-Cy5.5	SK7	BD
CD57 PE-Cy7	HNK-1	Biolegend
CD38 V450	HB7	BD
CD4 V450	RPA-T4	BD
CD4 APC-H7	SK3	BD
CD45 RO FITC	UCHL-1	BD
CD3 V450	UCHT1	BD
CD28 PE-Cy7	CD28.2	BD
CD38 APC	HIT2	BD
CD107a BV421	H4A3	BD Biosciences
TCR γδ-1 PE	11F2	BD
CD56 FITC	NCAM 16.2	BD
CD16 FITC	NKP15	BD

Supp. Table 2. List of mAbs used in mass cytometry

Antigen	Clone	Metal conjugate
CD160-AF647	BY55	N/A
CD56	REA196	113In
CD8A	RPA-T8	115In
CD57 # *	HCD57	139La
CD49d # *	9F10	141Pr
CD19	HIB19	142Ce
CD45RA # *	HI100	143Nd
CD69 # *	FN50	144Nd
CD4	RPA-T4	145Nd
Cy5 (For AF647detection)	CY5-15	147Sm
CD28 # *	CD28.2	148Sm
CD366 (Tim3)	7D3	149Sm
KLRG1 # *	SA231A	150Sm
CD39 # *	A1	151Eu
CD45RO # *	UCHL1	152Sm
CD62L # *	DREG-56	153Eu
CD137 (41BB)	4B4-1	155Gd
CD279 (PD-1) # *	EH12.2H7	156Gd
CD197 (CCR7) # *	150503	159Tb
CD223 (Lag3)	17B4	160Dy
CD122 (IL-2RB)	TU27	161Dy
Vβ 21.3 *	IG125	162Dy
CD183 (CXCR3)	REA232	163Dy
CD274 (PDL1)	MIH1	164Dy
Vβ 8 *	56C5.2	165Ho
TIGIT #	MBSA43	166Er
CD27 #	M-T271	167Er
CD25	M-A251	169Tm
CD3	UCHT1	170Yb
CD38 #	HIT2	172Yb
Integrin B7	FIB504	173Yb
Vβ 5.1 or Vβ 13.1 *	IMMU157 or IMMU222	174Yb
CD127 # *	A019D5	176Lu
EOMES	WD1928	146Nd
Ki67	B56	168Er
Granzyme B	GB11	171Yb
Perforin	B-D48	175Lu
T-bet	4B10	209Bi

#Antigen used for FlowSOM clustering; *Antigen used for tSNE analysis; N/A, Not applicable.

Vuckovic et al. Supplementary Figures

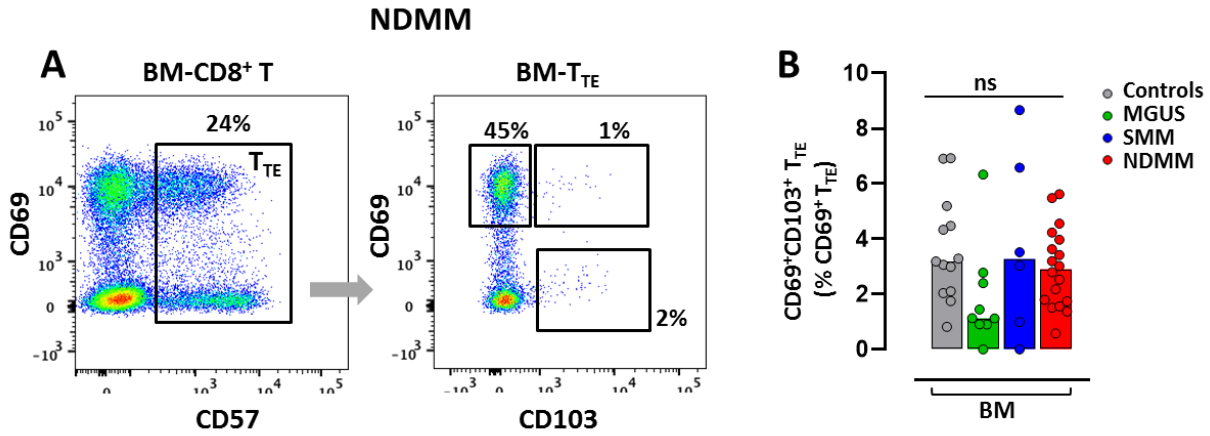

Supplementary Figure 1. **Expression of CD103 on BM-CD69^{+}T$_{TE}$. (A)** Representative dot plot show expression of CD69 and CD103 on BM-CD57^{+}T$_{TE}$ cells in a NDMM patient. **(B)** Bars (median with scatter plots) show the proportion of CD69^{+}CD103^{+} T$_{TE}$ cells within CD69^{+}T$_{TE}$ cells in the BM of controls (n = 14), MGUS (n = 9), SMM (n = 6) and NDMM (n = 18) patients. (Kruskal-Wallis test with Dunn's multiple comparisons; ns, not significant).

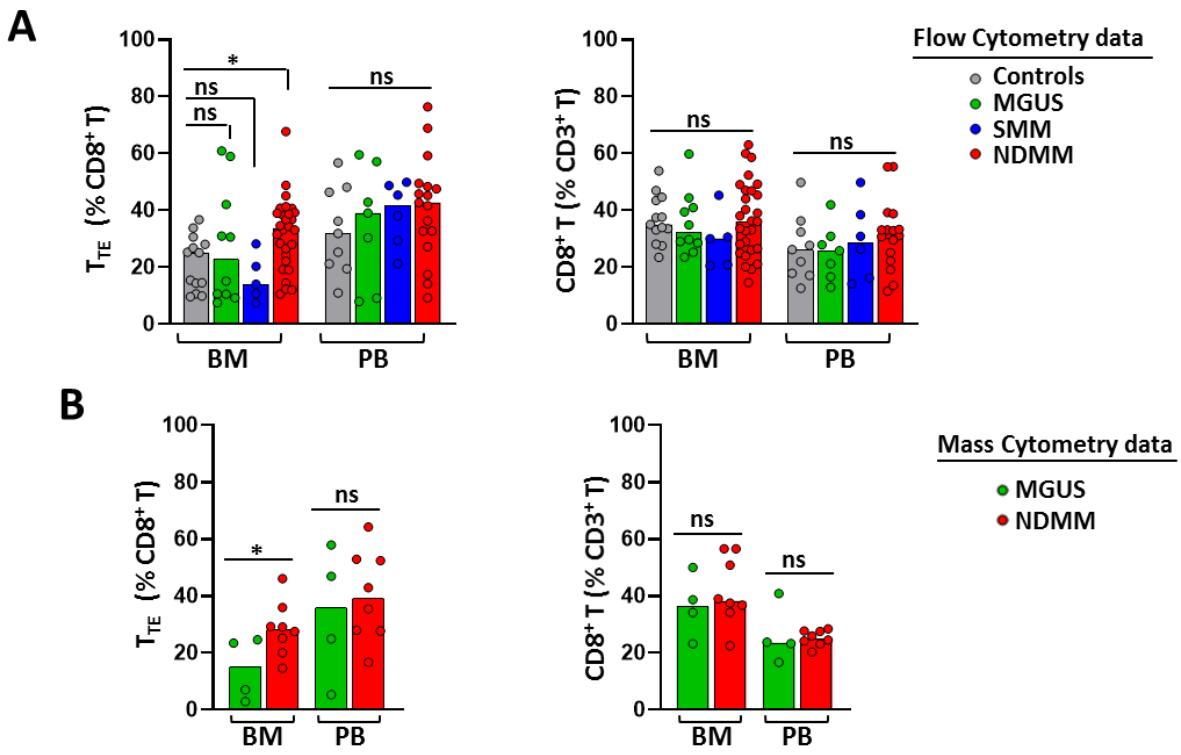

Supplementary Figure 2. Proportions of total T_{TE} and $CD8^+$T cells in the BM and PB of controls, MGUS, SMM and NDMM patients. (A) Fluorescence flow cytometry data, **(B)** Mass cytometry data. **(A)** Bars (median with scatter plots) show proportions of T_{TE} and $CD8^+$T cells in the BM of controls (n = 13), MGUS (n = 10), SMM (n = 5) and NDMM (n = 28) and PB of controls (n = 9), MGUS (n = 7), SMM (n = 6) and NDMM (n = 17). (Kruskal-Wallis test with Dunn's multiple comparisons; * $p < 0.05$; ns, not significant). **(B)** Bars (median with scatter plots) show proportions of T_{TE} and $CD8^+$T cells in the BM and PB of NDMM (n = 8) and MGUS patients (n = 4). (Mann Whitney test; * $p < 0.05$; ns, not significant).

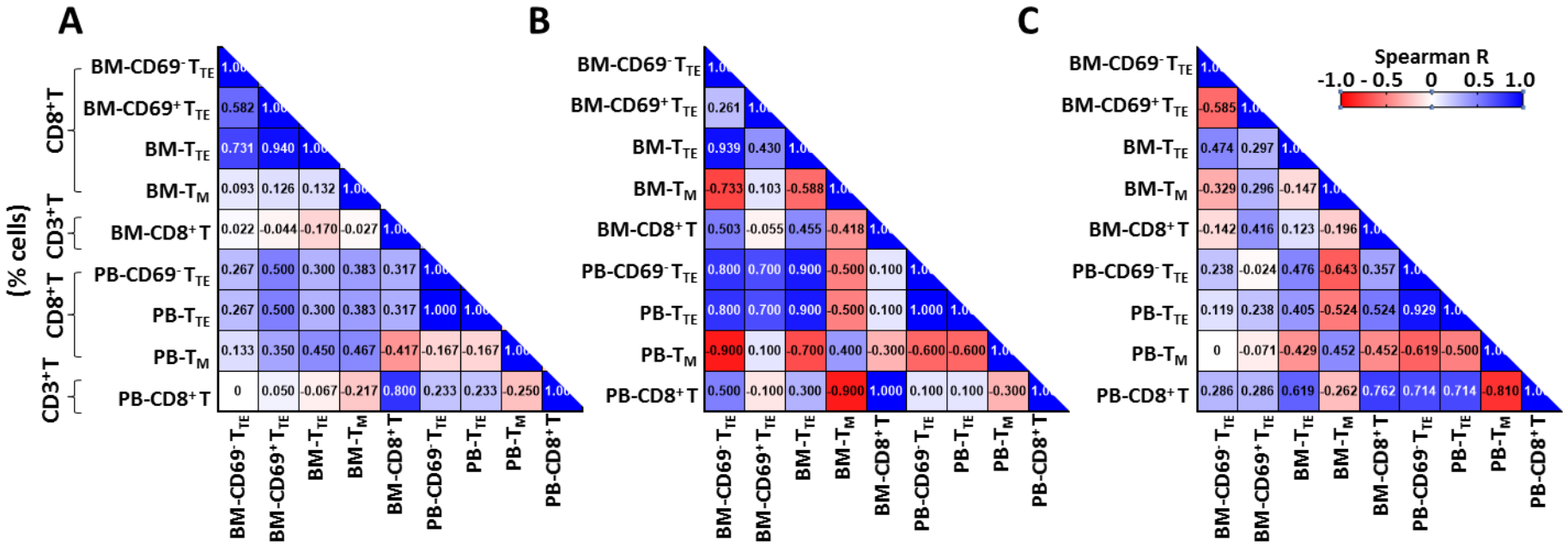

Supplementary Figure 3. Relationships between proportions of $CD69^{-}T_{TE}$, $CD69^{+}T_{TE}$, $T_{TE,}$ T_{M} and $CD8^{+}$T cells in controls, MGUS and NDMM patients. (A-B) The matrix shows correlations between proportions of $CD69^{-}T_{TE,}$ $CD69^{+}T_{TE}$, $T_{TE,}$ T_{M} ($CD8^{+}CD45RO^{+}CD57^{-}$) and $CD8^{+}$T cells in the BM and PB of **(A)** controls, **(B)** MGUS and **(C)** NDMM patients. Proportions of $CD69^{-}T_{TE,}$ $CD69^{+}T_{TE}$, T_{TE} and T_{M} are presented as % $CD8^{+}$T cells and proportion of $CD8^{+}$T as % $CD3^{+}$T cells (also shown in Fig. 2A-C). Each cell within matrix is labeled with corresponding Spearman R values.

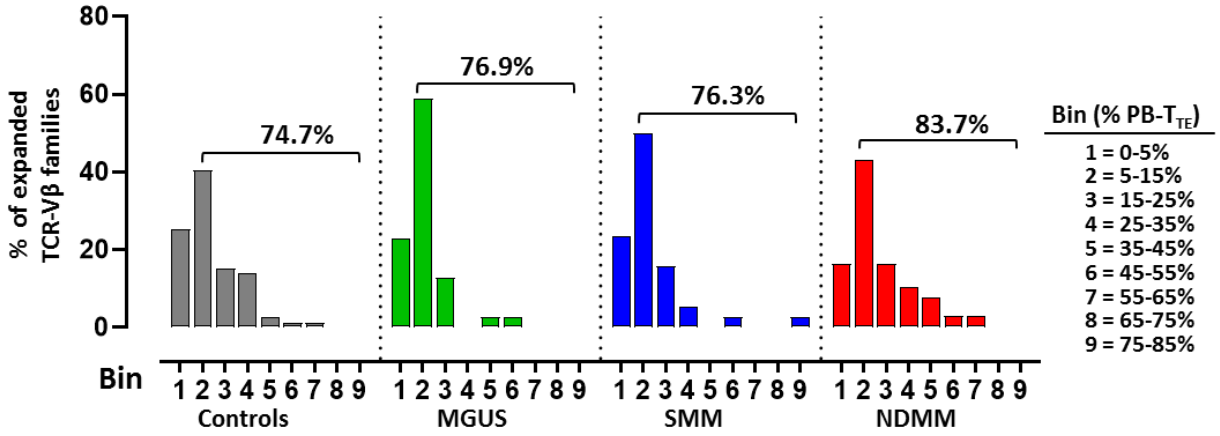

Supplementary Figure 4. Oligoclonal expansions within PB-T_{TE} of Controls, MGUS, SMM and NDMM. Plot shows the size distribution of expanded TCR-Vβ family-expressing populations within PB-T_{TE} in controls, MGUS, SMM and NDMM patients (also shown in Fig. 3A). Numbers indicate proportions of expanded TCR-Vβ family above an empiric cut-off of 5% of PB-T_{TE} cells.

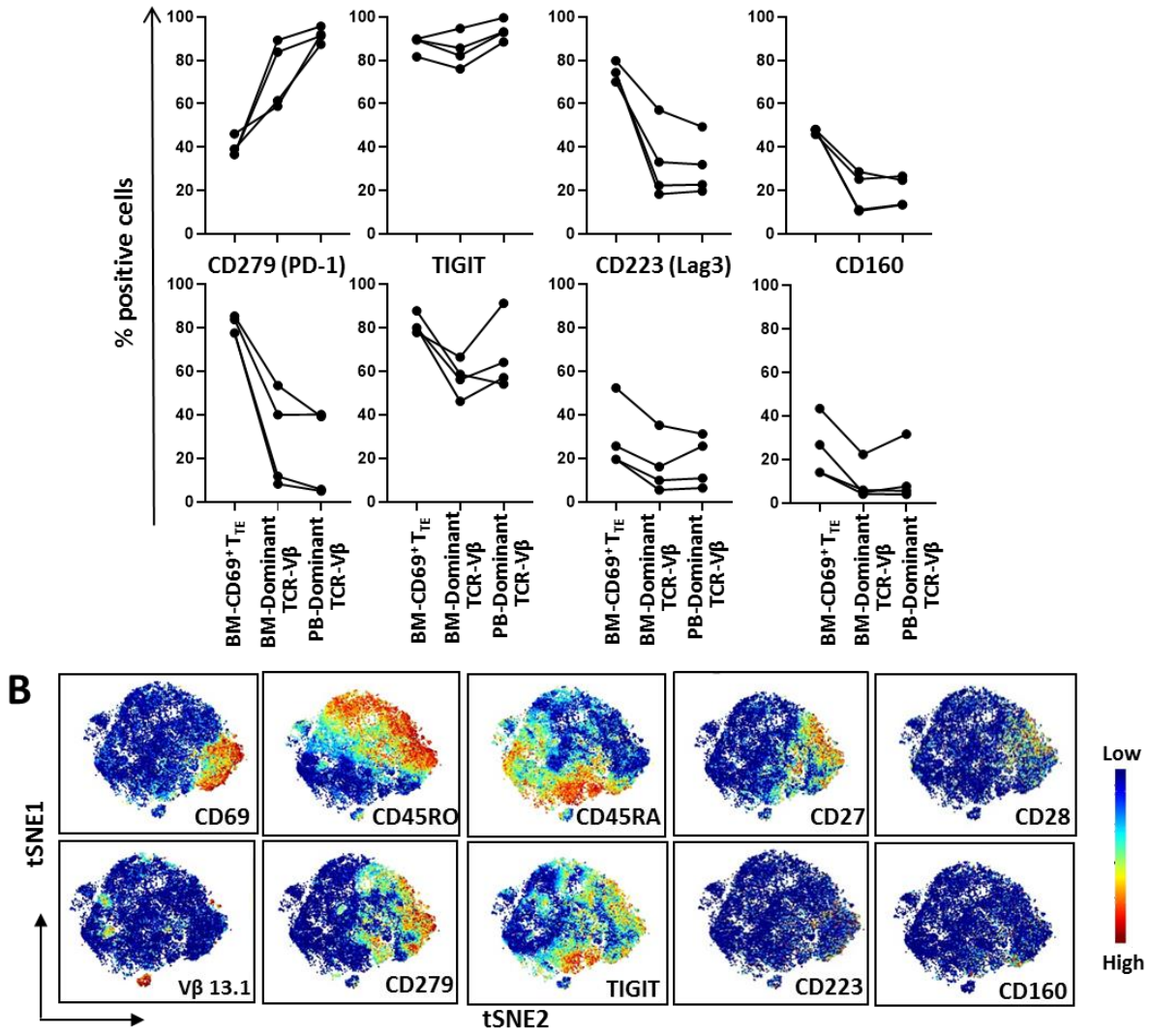

Supplementary Figure 5. Phenotype of BM-CD69^{+}T$_{TE}$ cells and CD69^{-}T$_{TE}$ cells expressing dominant TCR-Vβ in the BM and PB of NDMM patients defined by mass cytometry. (A) Proportion of cells expressing the indicated antigen within BM-CD69^{+}T$_{TE}$ and BM-T$_{TE}$ and PB-T$_{TE}$ expressing dominant TCR-Vβ families. Cells from individual NDMM patients are connected by a line. Data were obtained by manual gating of mass cytometry data using FlowJo software version 10.0.8r1. **(B)** tSNE plots show the distribution of the indicated antigen within pooled BM-T$_{TE}$ cells of NDMM patients (n = 5).